Geomechanics and Engineering, *Vol. 38, No. 4 (2024) 397-408*
https://doi.org/10.12989/gae.2024.38.4.397

Performance evaluation of underground box culverts under foundation loading

Bin Du*[1], Bo Hao[2], Xuejing Duan[3], Wanjiong Wang[2] and Mohammad Roohani[4a]

[1]*Civil & Architecture Engineering Xi'an Technological University, Xi'an, Shaanxi 710062, China*
[2]*School of Mechanical Engineering and Automation, Northeastern University; Shenyang, Liaoning, 110819 China*
[3]*Marine Engineering Department, Weihai Marine Vocational College; Rongcheng Shandong, 264300 China*
[4]*Faculty of Geotechnical Engineering, Civil Engineering Department, University of Zanjan, Zanjan, Iran*

(*Received April 20, 2024, Revised August 1, 2024, Accepted August 6, 2024*)

Abstract. Buried box culverts are crucial elements of transportation infrastructure. However, their behavior under foundation loads is not well understood, indicating a significant gap in existing research. This study aims to bridge this gap by conducting a detailed numerical analysis using the Finite Element Method and Abaqus software. The research evaluates the behavior of buried box culverts by examining their interaction with surrounding soil and the pressures from surface foundation loads. Key variables such as embedment depth, culvert wall thickness, concrete material properties, foundation pressure, foundation width, soil elastic modulus, and friction angle are altered to understand their combined effects on structural response. The methodology employs a validated 2D numerical model under plane strain conditions. Parametric studies highlight the critical role of culvert depth (H) in influencing earth pressure and bending moments. Foundation pressure and width demonstrate complex interdependencies affecting culvert behavior. Variations in culvert materials' elastic modulus show minimal impact. It was found that the lower wall of the buried culvert experiences higher average pressure compared to the other two walls, due to the combined effects of the culvert's weight and down drag forces on the side walls. Furthermore, while the pressure distribution on the top and bottom walls is parabolic, the pressure on the side walls follows a different pattern, differing from that of the other two walls.

Keywords: bending moment; box culvert; earth Pressure; foundation loading; numerical analysis

1. Introduction

Embedded beneath the earth's surface, buried box culverts play a pivotal role in civil engineering endeavors. These structures, vital for traversing roads and railways over streams and drainage systems, subjected to diverse loads, resulting in soil-structure interaction that necessitates a profound understanding for the formulation of safe and cost-effective designs (Zheng and Li 2024, Jiao *et al.* 2024, Almasabha *et al*. 2023, Yoo *et al.,* 2022, Oh *et al.* 2019, Aziz *et al.* 2017, Terzi *et al.* 2015). The interaction between box culverts and the encompassing soil involves intricate considerations, including the structure's relative stiffness, the phenomenon of soil arching, and the impact of foundations loading on structural responses of buried box culvert (Wu *et al.* 2024, Jin *et al.* 2024, Li *et al.* 2023, Nawel and Salah 2015, Bryden *et al*. 2014). Soil arching, initially studied by Terzaghi (1943) and subsequently investigated by later scholars (Li *et al.* 2014, Spangler 1950) adds intricacies to the stress redistribution process as a result of the existence of a stiff structure within a much less stiff medium. This phenomenon can either escalate or alleviate loading on the structure based on the relative stiffness between the soil and the buried culvert. The response of buried structures is complex, intensifying the challenge of predicting soil pressure distributions (Abuhajar Newson *et al*. 2015, Cheng and Li 2015, Liang and Bayrami 2023, Wang and Huang 2021). Moreover, positive and negative arching concurrently affecting the faces of the structure introduces more complexity. Reinforced concrete box culverts, commonly employed in various transportation infrastructures, face additional challenges when positioned in close proximity to roads, railways, or building foundations (Ahmad and Alarabi 2011, Maekawa *et al*. 2016). The presence of surface foundations induces varying soil pressures, potentially causing increased deformations and structural failures (Esmaeili-Falak and Sarkhani Benemaran 2023). As a consequence, evaluating the impact of surface foundations on box culvert responses becomes indispensable for ensuring their structural integrity (Abuhajar *et al*. 2015b, Abuhajar, Newson *et al*. 2015, Esmaeili-Falak and Sarkhani Benemaran 2024). Empirical studies on the soil pressure distribution over box culverts under embankment installations have contributed valuable insights (Abuhajar *et al*. 2015a, Chen *et al*. 2009, Moradi *et al*. 2022). Early works by Binger (1947), Spangler (1950), Spangler and Handy (1973), Terzaghi (1943) and others have shed light on soil pressure distribution characteristics, often identified as parabolic on the top wall of buried structure, with a high earth pressures at the edges and lower

*Corresponding author, Professor
E-mail: dubin@xatu.edu.cn
[a]Ph.D. Candidate
E-mail: mohammad.roohani2022@gmail.com

http://www.techno-press.org/?journal=gae&subpage=7
ISSN: 2005-307X (Print), 2092-6219 (Online)

pressure at the center (Hassankhani *et al*. 2016, Moradi *et al*. 2020, Pimentel *et al*. 2009). Numerical modeling research, such as that conducted by (Abuhajar *et al*. 2015b, Abuhajar *et al*. 2016), Stone and Newson (2022), and Orton (2015), has provided crucial insights into the effects of different parameters. However, there remains a need for further studies to corroborate and supplement these findings. Research performed on studying soil-culvert interaction (SCI) problems is relatively limited, with a scarcity of studies exploring the influence of surface foundations on buried structures. Empirical studies examining the impact foundation loading and traffic loads on box culverts (Abuhajar *et al*. 2015b, Awwad *et al*. 2000) are reported but left some questions unanswered. Acharya (2014) conducted experimental investigations into the influence of traffic loading on shallow buried box culverts, scrutinizing factors such as traffic load values, distance of truck axes, and speed of load movement. Numerical studies further explored the influence of concrete pavement thickness, fill depth, and culvert span on load distributions over the culvert (Acharya *et al*. 2016).

The importance of applied pressure on buried culverts brought a few installation methods into the practical works, including Induced Trench Installation (ITI). Induced Trench Installation is a construction technique used to reduce the vertical pressure exerted on buried structures such as pipes and culverts. This method involves creating a trench above the buried structure, backfilling it with lightweight or compressible materials, and then covering it with soil (McAffee and Valsangkar 2005). The lightweight materials in the trench help distribute the load more evenly, effectively reducing the pressure directly applied to the structure below. This technique creates a positive arching effect by decreasing vertical stress and increasing horizontal stress within the backfill, leading to a significant reduction in earth pressure on culverts installed beneath high embankments (Hassankhani and Esmaeili-Falak 2024). Studies have shown that induced trench construction not only decreases the stresses acting on culverts but also enhances the overall performance of the soil-geofoam-culvert system, particularly under cyclic loading conditions (Tafreshi *et al*. 2012). By utilizing the induced trench method, culverts experience reduced contact pressure on their walls, ensuring their structural integrity and longevity in challenging environments (Sun *et al*. 2011).

In recent studies, researchers delved into the response of box culverts to static surface loading caused by man-made embankments and loads exerted due to the building construction. experimental tests and numerical analyses were employed, conducting investigations to explore the effect of foundation location on soil-culvert interaction (SCI) (Al-Zaidee *et al*. 2020, Johnson 2023, Sukamta *et al*. 2023). The results, presented in terms of transferred soil pressure to the top wall of buried box culvert, and soil-structure interaction coefficient, contribute to proposing a methodology for quantifying earth pressure applied on the buried culvert (Katona and Vittes 1982, Kim and Yoo 2005, Pimentel *et al*. 2009).

Despite existing literature delving into the behavior of box culverts and examining various factors such as soil-structure interaction, surface foundations, and load distributions, there are still significant gaps, particularly in the investigation of how buried structures respond to variations in geometrical and geotechnical parameters. This includes considering the top, side, and bottom walls of box culverts. This study aims to bridge these gaps, adopting numerical modeling approach for a holistic understanding of buried box culverts subjected to applied pressure loads. In pursuit of this objective, an exploration into the geotechnical and structural aspects of box culverts is undertaken. This investigation specifically focuses on the transferred earth pressure affecting its three walls and the development of bending moments in each. Parametric analyses are conducted to investigate these aspects, with the numerical model validated against well-documented experimental results from the literature.

2. Methodological approach

In the pursuit of a comprehensive understanding of the behavior of buried box culverts subjected to foundation loads, numerical analyses were undertaken using the Finite Element Method (FEM) through the powerful Abaqus software (ABAQUS, ver. 2018). Abaqus has demonstrated its capabilities in solving complex geotechnical engineering problems and was chosen for its versatility and success in various modeling scenarios (Hassankhani and Halabian 2018, Helwany 2007, Hügel *et al*. 2008), aligning seamlessly with the objectives of this study. The decision to conduct the analysis in 2D, assuming a plane strain condition, was a deliberate choice to accommodate the typical elongated nature of buried culverts, a prevalent scenario in practical geotechnical problems. This approach allowed for a detailed examination of the structural response while optimizing computational efficiency.

The numerical model consisted of three main components: 1) a cohesionless soil representing the backfill material, simulated using the Mohr-Coulomb constitutive model, 2) a buried box culvert made of concrete and modeled with linear elastic behavior, and 3) a simplified representation of the foundation, characterized by a uniform pressure with limited width applied on the backfill surface above the buried culvert. This approach is aligned by the foundation behavior adopted in the experimental study conducted by Abuhajar, as a rigid footing was placed on the soil surface. This simplified representation of the foundation aimed to streamline the analysis while maintaining essential characteristics of the loading conditions.

Meshing, involved the use of 8-noded biquadratic plane strain quadrilateral elements (CPE8R) for the soil and 3-noded quadratic beam elements (B22) for the box culvert. These elements are introduced in ABAQUS library and successfully applied in many simulations (Hassankhani and Halabian 2018, Kim and Yoo 2005). The selection of these elements was driven by their specific characteristics, optimizing the accuracy of the simulation by effectively capturing the complexities within the soil and culvert components. The interaction between the soil

Table 1 Soil properties of Nevada sand (Sourced from (Abuhajar *et al*. 2016))

Mass Density (kg/m^3)	Elastic Modulus (MPa)	Poisson's Ratio	Friction Angle (°)	Cohesion (kPa)	Dilation Angle (°)
1688	30	0.3	32	0	8

Table 2 Geometrical and Mechanical Properties of buried culvert (Sourced from (Abuhajar *et al.* 2016))

Mass Density (kg/m^3)	Elastic Modulus (GPa)	Poisson's Ratio	Thickness, tc (m)	Width, Bc (m)	Embedment Depth, H (m)
2584	25.2	0.2	0.53	4.57	7.62

and culvert was meticulously modeled using interface simulation, introducing a value of 0.67 φ, where φ is the internal friction angle of the backfill material. This parameter choice was grounded in references supporting its appropriateness for modeling the sand-concrete interface (Hassankhani 2020, Liang and Bayrami 2023, Xenaki and Athanasopoulos 2001), allowing controlled sliding and separation between the soil and the culvert. The failure criteria wherein the interacted surfaces start to move is based on Mohr-coulomb criterion. Simulating the foundation pressure involved a gradual increase in uniform pressure until reaching the desired magnitude, replicating realistic loading conditions.

To establish the in-situ stresses within the soil medium and around the buried culvert, the initial phase of the numerical simulation involves defining gravity loading without any additional loads. This step sets up the natural stress state of the soil and the culvert under their own weight. In subsequent phases, the footing pressure is introduced and gradually applied to the soil surface. This staged approach ensures that the initial stress conditions are accurately captured before adding the external loads from the footing, allowing for a more precise analysis of the soil-culvert interaction under the combined effects of gravity and footing pressure.

The adoption of a base model served as the first step, providing validation through a comparison with experimental results from a well-documented study available in the literature. The validation of numerical analyses ensured the accuracy and reliability of the numerical model. Following successful validation, parametric studies were initiated, varying multiple parameters to explore the buried culvert's response comprehensively. These studies assessed the average earth pressure and maximum bending moments developed in each wall of the buried box culvert under different conditions, shedding light on its structural behavior and informing engineering design practices.

3. Verification of numerical modeling

Validation of the numerical analysis in this study drew upon experimental tests conducted by Abuhajar (2016). Abuhajar's experimental design involved burying a box culvert in Nevada sand, and the measurement of bending moments and soil pressures applied on the top wall of the box culvert was facilitated through tactile pressure sensors and strain gauges. The utilized backfill material in the experimental setup was fine, homogenous, and clean sand, characterized by particle sizes ranging from 0.075 to 0.550 mm, and classified as poorly graded (SP). The mechanical properties of soil are presented in Table 1.

The soil characteristics listed in this table have been derived from the Abuhajar study which conducted laboratory tests to determine the Nevada sand properties employed in his experiments. The box culvert, consisted of aluminum square tube, featured a wall thickness of 6.35 mm under centrifuge tests subjected to 60g acceleration, maintaining a 1:1 width-to-foundation width ratio. To simulate a footing pressure of 100 kPa for the prototype model, a strip foundation was employed in the centrifuge tests. Strain gauges and tactile pressure sensors strategically placed around the box culvert facilitated the measurement of bending moments and soil pressures. In replicating the behavior of the prototype model, the numerical model adjusted the culvert characteristics: Culvert width (B_c) was set to 4.57 m, box wall thickness (t_c) to 0.53 m, and culvert embedment depth (H) to 7.62 m. These values has been achieved regarding the 60 g acceleration employed in centrifuge tests conducted by Abuhajar *et al.* (2016). Table 2 provide information on the geometrical and mechanical properties of buried culvert for base model.

The numerical model employed a quadrilateral element for meshing, with a finer mesh size around the box culvert aiming to capture stress more smoothly and precisely, regarding the expected stress concentration around the buried box. A distance of $4B_c$ for placing lateral and bottom boundaries was found appropriate so as to avoid impacting stress distribution patterns within the soil medium. The lateral boundaries were constrained in horizontal direction but free to move vertically. The bottom boundary was fixed in both horizontal and vertical directions to simulate fixed boundary.

In the meshing process of the base model, the soil medium was divided into 1,696 quadrilateral elements, while the culvert itself was represented using 72 beam elements. To ensure accurate modeling, the elements surrounding the buried culvert were assigned a size of 0.25 meters. In contrast, the maximum size of the elements near the lateral boundaries of the model was set to 2 meters. For the culvert, a mesh size of 0.25 meters was chosen, matching the size of the adjacent soil elements for consistency. Fig. 1 illustrates the finite element meshing, boundary condition and geometry of the model.

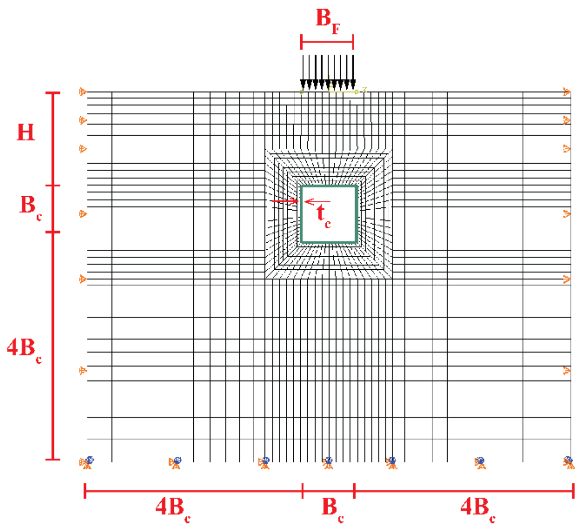

Fig. 1 Model Geometry and Finite Element Meshing

The results of the numerical analysis for the base model, compared with experimental measurements, considering the transferred pressure and developed bending moment in the top wall of the buried box culvert subjected to a foundation pressure of 100 kPa. The analysis revealed a distinctive hyperbolic distribution of pressure on the top wall, characterized by the lowest values at the mid-span and a gradual increase towards the edges. Both numerical results and sensor measurements corroborate this pattern. The calculated pressure at the axis line of the buried box closely aligns with the measured value, with a difference of less than 3%. However, by approaching the culvert corners, a slight discrepancy arises. The maximum calculated pressure differs just above 3% from the maximum measured pressure obtained from the experimental test. Despite these variations, it can be asserted that, on the whole, both experimental and numerical results exhibit good agreement.

Turning to the analysis of developed bending moments, a notable concurrence is observed between computed and measured values. The computed values fit well with the experimental values, capturing the intricate pattern of bending moment distribution in the top wall. The range of bending moments spans from a minimum of -119.3 kN. m to a maximum of 164.4 kN. m, indicating a tendency for the top wall slab to deform in a concave form for negative values and in a convex form for positive values. The zero value for bending moments signifies the location of the inflection point of the slab.

Considering the mean values, the average pressure on the top wall, as depicted in Fig. 2, is calculated to be 160.1 kPa. Simultaneously, the average bending moment is -119.3 kN. m, indicating that a substantial portion of the top wall slab experiences a depressed deformation. These results contribute valuable insights into the structural response of the buried box culvert, providing a basis for further discussions on the observed behavior in later sections and potential design considerations.

To provide a more comprehensive understanding of the stress distribution around the buried culvert, Fig. 3 has been included, serving as a foundational element for subsequent

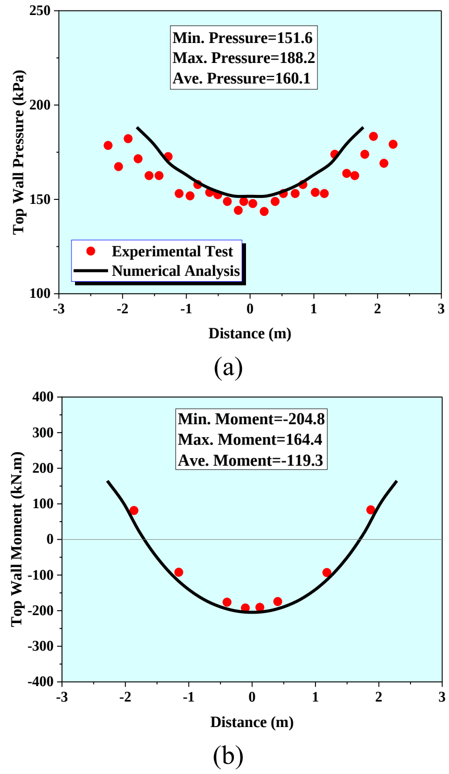

Fig. 2 Comparison of experimental and numerical results of (a) transferred pressure and (b) bending moment in top wall of buried box culvert

discussions. The stress contours depicted in this figure exhibit significant variations around the buried culvert. Analyzing the vertical stress distribution, it becomes apparent that the pressure values along a horizontal level just above the culvert are lower than those at greater distances away from the culvert. This proves that the culvert's top wall undergoes less pressure compared to a point at the same depth but further away from the culvert. Regarding the stress distribution on the bottom wall, as illustrated in Fig. 3(a), it is evident that the lower slab experiences higher pressure than the upper wall.

This observation can be attributed to the weight of the culvert and the down drag forces on the side walls, which exert downward pressure and result in higher pressure on the bottom wall. Similar to the top wall, the pressure distribution on the bottom wall is non-uniform, with the lowest and highest values occurring at the middle and edges of the slab. Fig. 3(b) illustrates the applied lateral earth pressure on the side wall of the culvert, highlighting values at several points. Unlike the parabolic pattern observed for top and bottom walls, the pressure distribution on the side wall does not follow a parabola. The lower corner undergoes the maximum pressure, reaching 68.1 kPa, while the upper corner experiences the minimum pressure, equal to 28.7 kPa. Fig. 4 provides a detailed depiction of the bending moment distribution in all three walls of the box culvert. Notably, the results highlight that the bending moment values developed in the bottom wall surpass those in the other slabs. At the mid-span of the bottom wall, a substantial bending moment of -298 kN. m is observed,

Table 3 Transferred pressure and developed bending moments in top, bottom and side wall of buried box culvert

	Applied Pressure (kPa)			Bending Moment (kN. m)			
	Minimum	Maximum	Average	Minimum	Maximum	Average	Maximum of Absolute values
Top Wall	151.6	188.2	160.1	-204.8	164.4	-119.3	204.8
Bottom Wall	216.8	305.5	226.5	-298	214	-126.2	298
Side wall	28.7	68.1	50.5	56	214	122.8	214

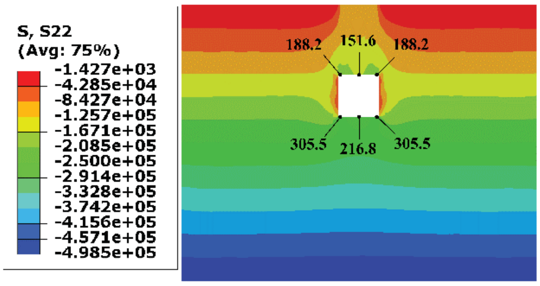

(a) Vertical stress

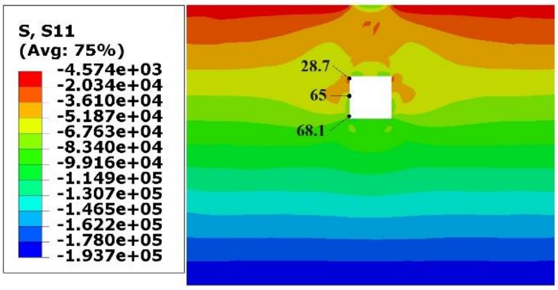

(b) Horizontal stress

Fig. 3 Vertical stress and Horizontal stress distribution within the backfill and around the buried culvert (the legend values are in Pa and values shown on figure are in kPa

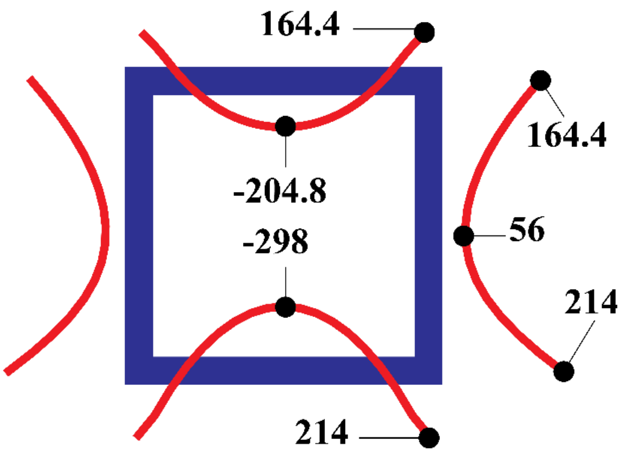

Fig. 4 Distribution of bending moment in walls of box culvert (values in kN.m)

originating from the middle of this wall and extending to the value of 214 kN. m at the two corners. It is noteworthy that this value is equal to the moment at the lower point of the side wall. An intriguing observation is the distinction in the nature of bending moments across different walls. While both positive and negative moments occur at the top and bottom walls, the side wall exclusively experiences positive values. This indicates that the deformation of the side wall is convex along its length.

Table 3 presents a summary of the numerical analysis results for the base model, illustrating the minimum, maximum, and average values of applied pressure and bending moments in the three walls of the buried box culvert. The focus on average values aligns with guidelines and standards that primarily address the mean pressure of earth pressure. In terms of applied pressure, the average values are particularly relevant for this study. The table reveals that the bottom wall experiences the highest average earth pressure, while the side wall bears the lowest mean pressure among the three walls. Turning to bending moments, the criterion for consideration is the maximum of absolute values, as structural design considerations for culverts typically prioritize the maximum bending moment irrespective of its sign. Similar to the applied pressure, the bottom wall registers the highest value of bending moment. Following closely, the side wall experiences the second-highest bending moment. It's worth noting that the maximum bending moment in the side wall occurs at the lower point, equivalent to the bending moment at the edge of the bottom wall.

These obtained results serve as a foundational basis for the subsequent analysis. In the forthcoming assessments, the focus will be specifically on the mean pressure values and the maximum of absolute bending moments. This targeted approach aims to provide a comprehensive understanding of the buried box culvert's response, emphasizing the significance of average pressure conditions and the extreme values of bending moments. Such a selective consideration aligns with industry standards and design practices, allowing for a more nuanced evaluation of the structural behavior and performance of the buried box culvert under varying conditions.

4. Studied parameters

While the base model concentrated solely on the pressure distribution and bending distribution of the top wall of the buried culvert, the broader numerical analysis encompassed the behavior of all walls—top, side, and bottom. This comprehensive approach ensures a holistic understanding of the buried culvert's response under varying conditions, contributing to the applicability and relevance of the study's findings in practical geotechnical engineering scenarios.

The variables selected for parametric studies are organized into three main components of the investigated problem: culvert, foundation, and backfill soil. Specifically,

Table 4 Studied parameters and corresponded range

	Box Culvert			Found ation		Soil	
Variable	Embedment Depth, H (m)	Wall's Thickness, t_c (m)	Elastic Modulus, E_c (GPa)	Foundation Pressure, P_0 (kPa)	Foundation Width, B_F (m)	Friction Angle, φ(Degree)	Elastic Modulus, E_s (MPa)
Studied Range	1.0~15.0	0.1~1.0	21.0~31.5	50~1000	6.2~20.0	25~45	10~100

for the culvert, the explored parameters are the embedment depth, wall thickness, and elastic modulus of the concrete material. The foundation was characterized by two primary parameters—foundation pressure and foundation width. In the case of backfill soil, the internal friction angle and elastic modulus of the soil were the variables under study. Table 4 provides a comprehensive overview of the studied variables, including the range of each parameter considered in the parametric studies. The chosen ranges align with typical values relevant to practical applications. It is essential to note that, during parametric studies, emphasis was placed on two key aspects: the average pressures applied on culvert walls and the maximum of absolute values of bending moments developed in each wall. These results have been effectively visualized in the form of graphs. Throughout the parametric studies, only the variable under investigation was varied, while other parameters were maintained identical to the base model. Additionally, the presentation of variables in the form of nondimensional parameters was prioritized to facilitate a more generalized and applicable understanding of the study outcomes.

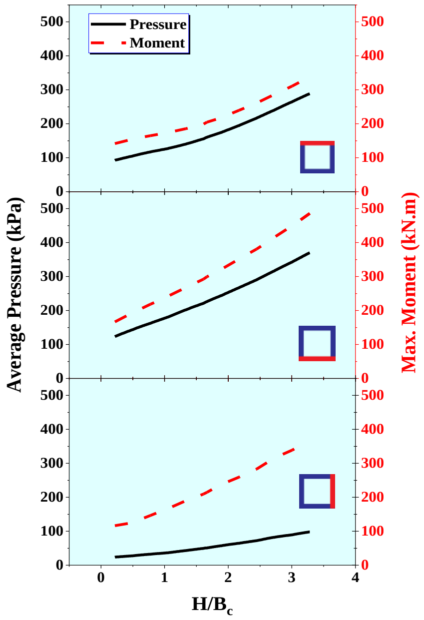

Fig. 5 Effect of culvert embedment depth (H) on the response of various walls of buried box culvert

5. Results and discussion

5.1 Culvert characteristics

In this section, a comprehensive numerical investigation is undertaken to explore various parameters associated with a buried box culvert. The parameters subjected to variation include the embedment depth (H), the thickness of the culvert walls (t), and the elastic modulus of the culvert material. The selected range for each parameter aligns with typical values, and the outcomes are methodically presented, focusing on the average transferred pressure to distinct walls of the buried box culvert and the maximum bending moment developed within the culvert walls. The influence of each parameter has been regarded in a nondimensional form.

Fig. 5 depicts the outcomes of the conducted analyses on the impact of buried embedment depth (H) on the resultant bending moment and average pressure acting on the top, side, and bottom walls of the buried box culvert under surface foundation pressure. Observations reveal a noteworthy increase in both average pressure and bending moments across all three walls with an augmentation in the H parameter, signifying the significant influence of embedment depth on the culvert's response. Notably, the pressure exerted on the side wall consistently registers lower values compared to the top and bottom walls. As the H value varies from 1 to 15 m (equivalent to H/B_C ranging from 0.22 to 3.3), the average pressure on the side wall ascends from 23 to 98 kPa. However, the applied earth pressure on the top and bottom walls increases from 92 to 288 kPa and 123 to 370 kPa, respectively. This demonstrates a roughly threefold increase for the top and bottom walls, whereas the side wall experiences more than 4-fold increase within the investigated H/B_C values. The higher-pressure values transferred to the top and bottom walls compared to the side wall can be attributed to two factors. Firstly, lateral earth pressure is less than vertical pressure due to the at-rest condition or potential active conditions, regarding the context of horizontal stresses. Secondly, the foundation surcharge applied above the buried box culvert has a more pronounced effect on the top wall and subsequently on the bottom wall. Another noteworthy observation is that the pressure on the bottom wall surpasses that on the top wall, which can be rationalized by the fact that the pressure on the bottom wall is a result of both the pressure applied to the top wall and the self-weight of the culvert. It is important to highlight that with increasing embedment depth, the weight of the soil column above the culvert rises, while the impact of foundation pressure diminishes. Nevertheless, the calculated pressures on the various walls exhibit an ascending trend, underscoring that the influence of soil weight is more prominent than the diminishing effect of foundation pressure.

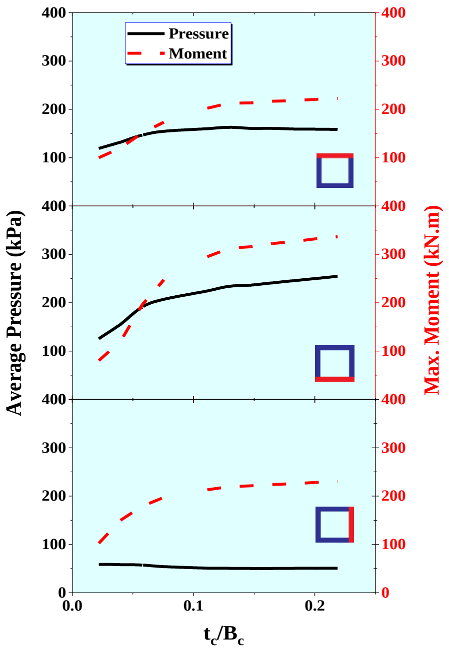

Fig. 6 Effect of culvert wall's thickness (t_c) on the response of buried box culvert

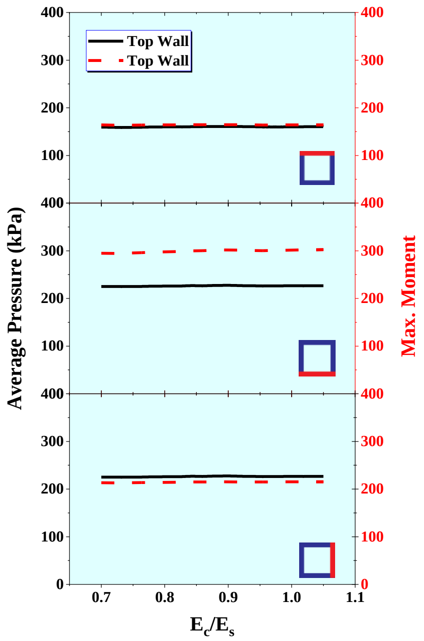

Fig. 7 Effect of elastic modulus of culvert material (E_c) on the response of buried box culvert

Concerning the computed maximum bending moment in distinct walls of the box culvert, an evident correlation emerges, mirroring the pattern of applied pressure for all three walls. Notably, this correlation is more pronounced for the top and bottom walls in comparison to the side wall. Delving deeper into the specifics, it is noteworthy that the maximum bending moment on the side wall exhibits a higher rate of increase than the average pressure applied to it. Taking a specific instance, when H/B_C equals 3, the calculated values for bending moments on the top, bottom, and side walls stand at 311, 449, and 339 kN · m , respectively. This highlights a substantial discrepancy, with the maximum bending moment in the bottom wall surpassing that of the other two walls of the culvert. Intriguingly, despite the lower average pressure exerted on the side wall, the developed maximum bending in the side wall exceeds that in the top wall. This peculiar observation can be rationalized by considering that the maximum bending moment in the side wall equals the bending moment at the edge of the bottom wall (the intersection of the bottom and side walls). At this corner, the bending moment is notably greater than the corresponding point on the upper wall and falls between the moments at the center of the top wall and the center of the bottom wall. One plausible explanation is rooted in the mechanics of load distribution within the culvert structure.

The calculated results emphasize the significant influence of culvert depth on the buried culvert's behavior. Specifically, an increase in embedment depth exerts a considerable impact on both the earth pressure and bending moments experienced by different walls of the box culvert. The findings from the investigation into the impact of culvert wall thickness, as depicted in Fig. 6, reveal noteworthy trends. It is essential to highlight that, for this study, all culvert walls share identical thickness. The selected range for the thickness (t_c) spans from 0.1 to 1.0 m, corresponding to t_c/B_Cratios between 0.02 and 0.22.

The figure illustrates a discernible increase in applied pressure on the top and bottom walls as t_c increases. This elevation in applied and bending pressure is attributed to the heightened stiffness resulting from thicker culvert walls, enabling the culvert to absorb more load and consequently leading to the development of larger bending moments. However, it is crucial to note that the rate of this increase diminishes when t_c/B_C surpasses 0.06, indicating a potential transition to a rigid state for t_c greater than 0.3 m. This specific point highlights a differential rate of increase in applied earth pressure for the top and bottom walls, with the bottom wall experiencing a greater rate due to the additional weight incurred by thickening the culvert walls. For t_c/B_C ratios exceeding 0.06, no significant changes in average pressure and maximum bending moment are observed in different sides of the box culvert. Despite the increasing trend for the upper and lower walls, the side wall experiences a decline in applied average pressure. However, this decrease is negligible, given the minimal changes associated with varying t_c . Conversely, the maximum bending moment in the side wall follows an increasing trend, influenced by the moments at the edges of the top and bottom walls of the buried culvert. overall, the analysis of culvert thickness indicates that, beyond a certain point, increasing wall thickness has an insignificant impact on the buried box culvert's response. This parameter exerts the least influence, particularly concerning the side wall, suggesting that a critical threshold for wall thickness is reached where further increase yields marginal effects on the culvert's behavior.

The examination of the influence of culvert materials, specifically concrete, involved varying the concrete elastic modulus (E_c) within the range of 21.5 to 31.5 GPa,

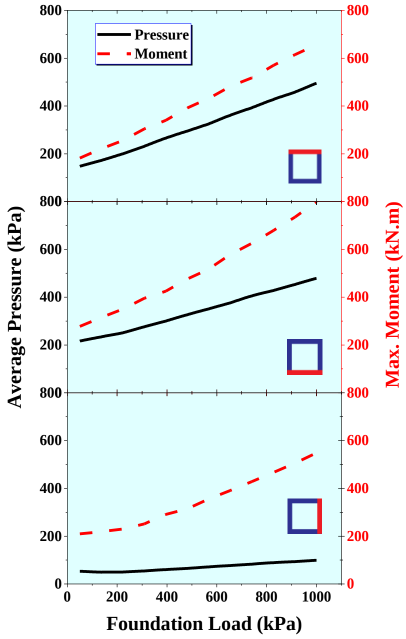

Fig. 8 Effect of foundation pressure (P_0) on the response of buried box culvert

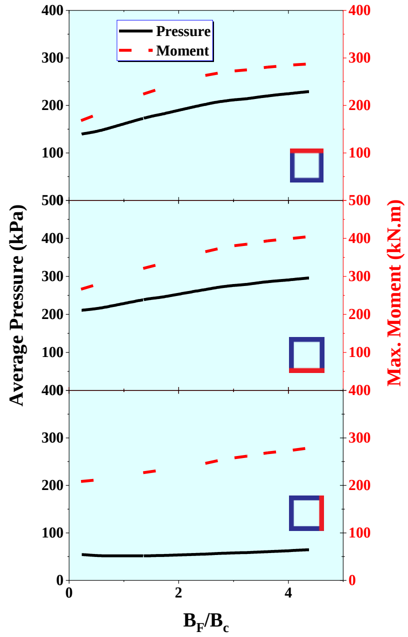

Fig. 9 Effect of foundation width (B_f) on the response of buried box culvert

representative of typical concrete materials. The results, as depicted in Fig. 7, indicate that E_c does not exert a significant effect on the buried culvert's response within the studied range. The figure illustrates that the maximum differences in applied pressure to various walls are less than 2 kPa. However, the side wall experiences a slight increase in maximum bending moment values, approximately 7 kN · m, when E_c is increased from 21.5 to 31.5 GPa. For a specific value of E_c/E_s=1.0, as an illustrative example, the maximum bending moments for the top, bottom, and side walls are determined to be 164, 301, and 215 kN · m, respectively.

This outcome aligns with the patterns observed in previous sections, wherein the maximum bending moment in the side wall is less than that in the bottom wall but greater than that in the top wall. Overall, the study concludes that, at least within the examined range, the variation in concrete elastic modulus does not significantly impact the response of the buried culvert, affirming the robustness of the culvert's performance under diverse material conditions.

6. Foundation characteristics

This section delves into the examination of foundation characteristics, specifically foundation width (B_f) and foundation pressure (P_0). It is pertinent to note that, in all cases, the foundation mid-axis aligns with the culvert mid-axis, ensuring symmetry with no deviation relative to the buried culvert's symmetry axis.

The impact of foundation pressure was investigated by varying P_0 values from 50 to 1000 kPa, as illustrated in Fig. 8. Notably, at the minimum foundation pressure of 50 kPa, the transferred pressure to the top, bottom, and side walls measured 147, 216, and 53 kPa, respectively, surpassing the foundation pressure. This counterintuitive observation is attributed to the influence of both vertical and horizontal stresses on various sides of the buried box, emphasizing that the magnitude of transferred pressure is more responsive to these stresses than the absolute value of the foundation pressure. As P_0 increases, the magnitude of transferred pressure also rises, but for large P_0 values, the pressure on the three sides becomes less than the foundation pressure. For instance, at the maximum foundation pressure (P_0=1000 kPa), the transferred pressure to the top and bottom walls is less than half of P_0, while for the side wall, it is notably lower, falling below $0.1P_0$. This unexpected trend, where the earth pressure exerted on the buried culvert becomes less than P_0 at higher foundation pressures, contradicts expectations based on the higher stiffness of the buried culvert relative to the surrounding soil. However, it is crucial to recognize that due to the deformation of culvert walls, the magnitudes of transferred pressure diminish, and this behavior is subsequently observed.

Examining the values of bending moments reveals a correspondence with the foundation pressure trend, indicating an increase in these values with rising P_0. When scrutinizing the side wall, the rate of increase in bending moment surpasses that of the top and bottom walls, emphasizing a more substantial influence. Despite the relatively smaller values of applied pressure to the side wall, this trend underscores that the maximum bending moment developed in the side wall is more influenced by bending moments in the bottom wall than the lateral earth pressure on this side of the buried box culvert. This behavior invites further exploration into the interplay of foundation pressure, lateral stresses, and culvert wall deformations.

In examining the influence of foundation width (B_f), variations were made from 1 to 20 m, corresponding to B_f/B_c ratios ranging from 0.22 to 4.4. Unsurprisingly, an increase in foundation width results in a corresponding rise in applied pressure to the culvert walls. However, it is noteworthy that the increase rate for the side wall is substantially lower compared to the other two walls, as depicted in Fig. 9. Even with an identical foundation pressure magnitude in all cases (P_0=100 kPa), the escalated transferred pressure to the buried culvert can be rationalized by the widening influence of B_f on the adjacent soil columns surrounding the culvert.

As B_F increases, the adjacent soil columns experience an increased influence of the foundation pressure, preventing the diversion of soil stresses from the column directly above the culvert to the adjacent columns. This phenomenon results in higher pressures on the top and bottom walls, exceedingly even the applied foundation pressure, as evident in Fig. 9. The augmented transferred pressure, regarding the limited foundation pressure, can be primarily attributed to the prevention of stress transfer from the soil column above the culvert to adjacent columns. Additionally, the buried culvert's higher stiffness relative to the soil contributes to attracting more load.

The trend of maximum bending moments aligns with the pattern of applied pressure to the culvert walls, consistent with earlier observations in previous sections. This correlation further emphasizes the interdependence of foundation width, transferred pressure, and resulting bending moments, providing valuable insights into the intricate dynamics governing the buried culvert's response to varying foundation characteristics.

7. Soil characteristics

In the course of this study, the backfill soil is assumed to exhibit characteristics of cohesionless soil. Given prior research that has indicated the negligible impact of parameters like Poisson's ratio on the development of arching above buried structures, the conducted investigation focuses primarily on two key soil parameters: the elastic modulus (E_s) and the internal friction angle (ϕ).

The elastic modulus, E_s, is varied within a range of 10 to 100 MPa, a range typically associated with sandy soil. It's noteworthy that the elastic modulus of the culvert material (E_c) remains constant at 25.2 GPa, a value consistent with the benchmark model. Fig. 10 graphically illustrates the outcomes of this investigation. The findings reveal that the stiffness of the backfill material, as represented by the elastic modulus (E_s), has a marginal effect on the applied soil pressure to different sides of the buried culvert. Even with a tenfold increase in the E_s/E_c ratio, ranging from 0.0004 to 0.004, the variations in average pressure on the top, bottom, and side walls are found to be less than 6%. Interestingly, a closer examination of the results indicates a slight decrease in the average pressure for the top and bottom walls with an increase in E_s. Conversely, the side wall experiences a slight increase in average pressure.

These behaviors are attributed to the altered distribution

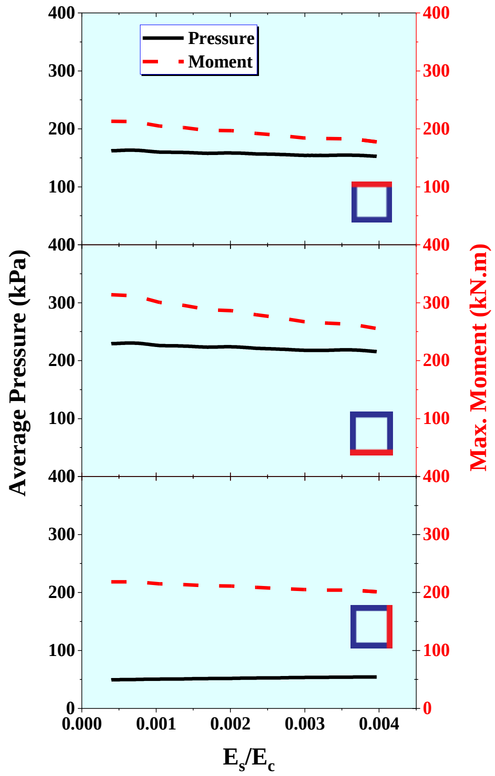

Fig. 10 Effect of soil elastic modulus (E_s) on the response of buried box culvert

of soil stresses, where the increased stiffness of the backfill, material diverts soil stresses from the soil column above the box towards adjacent soil columns. This shift in stress distribution contributes to an elevation in lateral earth pressure on the side wall.

Turning to the maximum bending moments developed in the upper and lower walls, it becomes evident that these follow a similar trend to the earth pressure but with a more pronounced rate of change. This accelerated pace is explained by the direct relationship between bending moments and the square of the beam length under pressure, a fundamental principle in structural mechanics. Notably, the side wall exhibits a reverse trend compared to the average pressure, indicating a dependency on the trend of moments in the bottom wall rather than the exerted average pressure.

The outcomes of investigating the impact of the internal friction angle of the backfill soil on the buried culvert's response are presented in Fig. 11. The results illustrate that with an increase in the friction angle, the applied pressure to all three sides experiences a corresponding increase, subsequently leading to a rise in maximum bending moments. Notably, the rate of growth in bending moment and average pressure is more pronounced when the friction angle increases from 25 to 33 degrees.

As the friction angle surpasses 33 degrees, its influence on the culvert response becomes negligible. In this range, further increases in the friction angle do not yield substantial changes in either average pressure or bending moments. This observation suggests a pivotal point in the

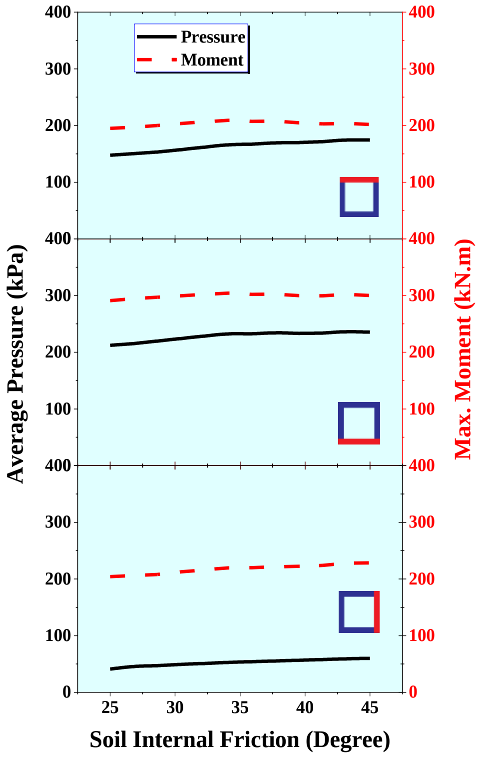

Fig. 11 Effect of soil friction angle (ϕ) on the response of buried box culvert

influence of the friction angle on the buried culvert's behavior, highlighting the importance of considering this critical soil parameter within an optimal range for effective design and analysis.

8. Conclusions

This study aimed to comprehensively investigate the behavior of buried box culverts subjected to foundation loads, focusing the transferred pressure and developed bending moments in different slabs of box culvert. The methodology involved finite element analyses using Abaqus software, with a focus on parameters such as culvert characteristics, foundation attributes, and soil properties. The obtained results could be summarized as below:

-Pressure follows a similar pattern on top and bottom walls, with the lowest values at the mid-span and gradually increasing towards the edges. The lower wall experiences higher pressure than the top wall due to the culvert's weight and down drag forces, causing a distinctive distribution.

-Non-uniform and non-symmetrical pressure distribution on side walls were observed. Variations are attributed to the diversion of soil stresses from the soil column above the culvert and changes in vertical stresses along the side wall with increasing depth.

-Embedment depth significantly influences transferred pressure, with an increase leading to notable pressure increments. However, Wall thickness impact is just significant when t_c/B_c is less than 0.06, diminishing thereafter. Meanwhile, Culvert material elastic modulus shows negligible impact on the box culvert behavior.

-For low foundation pressures, transferred pressure exceeds foundation pressure, but this trend reverses as foundation pressure grows. Soil stress redistribution around the box culvert accounts for the shift in transferred pressure behavior.

-Elastic modulus of backfill soil has a negligible impact on box culvert behavior. In addition, soil friction angle influences transferred pressure and bending moments up to a certain value (33 degrees), beyond which its impact diminishes.

This study provides a foundational understanding of buried box culvert behavior, yet further investigations could delve into dynamic analyses and real-time monitoring to enhance the robustness of the findings. Additionally, exploring the impact of varying soil types and environmental conditions could contribute to a more comprehensive design framework for buried structures. Future research might also consider the incorporation of advanced materials and construction techniques to assess their potential influence on the structural response of buried box culverts.

References

ABAQUS. (ver. 2018), *Standard User's Manual*. In Dassault Systemes Simulia Corporation.

Abuhajar, O., El Naggar, H. and Newson, T. (2015a), "Experimental and numerical ivestigations of the effect of buried box culverts on earthquake excitation", *Soil Dyn. Earthq. Eng.*, **79**(1), 130-148. https://doi.org/10.1016/j.soildyn.2015.07.015.

Abuhajar, O., El Naggar, H. and Newson, T. (2015b), "Static soil culvert interaction the effect of box culvert geometric configurations and soil properties", *Comput. Geotech.*, **69**, 219-235. https://doi.org/10.1016/j.compgeo.2015.05.005.

Abuhajar, O., El Naggar, H. and Newson, T. (2016), "Numerical modeling of soil and surface foundation pressure effects on buried box culvert behavior", *J. Geotech. Geoenviron. Eng.*, **142**(12), 04016072. https://doi.org/10.1061/(ASCE)GT.19435606.0001567.

Abuhajar, O., Newson, T. and El Naggar, H. (2015), "Scaled physical and numerical modelling of static soil pressures on box culverts", *Can. Geotech. J.*, **52**(11), 1637-1648. https://doi.org/10.1139/cgj-2014-0493.

Acharya, R., Han, J., Brennan, J.J., Parsons, R.L. and Khatri, D.K. (2014), "Structural response of a low-fill box culvert under static and traffic loading", *J. Perform. Constr. Fac.*, **30**(1), 04014184. https://doi.org/10.1061/(ASCE)CF.1943-5509.0000690

Acharya, R., Han, J. and Parsons, R.L. (2016), "Numerical analysis of low-fill box culvert under rigid pavement subjected to static traffic loading", *Int. J. Geomech.*, **16**(5), 04016016. https://doi.org/10.1061/(ASCE)GM.1943-5622.0000652

Ahmed, A.O.M. and Alarabi, E. (2011), "Development formulation for structural design of concrete box culverts", *Pract. Period. Struct.Des. Constr.*, **16**(2), 48-55. https://doi.org/10.1061/(ASCE)SC.1943-5576.0000075.

Al-Zaidee, S.R., Alsalmani, A.H. and Salam, A. (2020), "Effects of soil-structure interaction and different simulation on the response of concrete box culverts", *IOP Conference Series: Materials Science and Engineering.*, https://doi.org/10.1088/1757-899X/901/1/012009.

Almasabha, G., Shehadeh, A., Alshboul, O. and Al Hattamleh, O. (2023), "Structural performance of buried reinforced concrete pipelines under deep embankment soil", *Constr. Innov.*, https://doi.org/10.1108/CI-10-2021-0196.

Awwad, E., Mabsout, M., Sadek, S., and Tarhini, K. (2000), "Finite element analysis of concrete box culverts", In *Computing in Civil and Building Engineering (2000)*, 1051-1053. https://doi.org/10.1061/40513(279)136.

Aziz, M., Khan, T.A. and Ahmed, T. (2017), "Spatial interpolation of geotechnical data: A case study for Multan City, Pakistan", *Geomech. Eng.*, **13**(3), 475-488. https://doi.org/10.12989/gae.2017.13.3.475.

Bennett, R.M., Wood, S.M., Drumm, E.C. and Rainwater, N.R. (2005), "Vertical loads on concrete box culverts under high embankments", *J. Bridge Eng.*, **10**(6), 643-649. https://doi.org/10.1061/(ASCE)1084-0702(2005)10:6(643).

Binger, W. (1947), "Discussion to 'Underground conduits—An appraisal of modern research'", *Proc. Am. Soc. Civ. Eng.*, https://doi.org/10.1061/TACEAT.0006164.

Bryden, P., El Naggar, H. and Valsangkar, A. (2014), "Soil-structure interaction of very flexible pipes: Centrifuge and numerical investigations", *Int. J. Geomech.*, **15**(6), 04014091. https://doi.org/10.1061/(ASCE)GM.1943-5622.0000442.

Cheng, Q.Y. and Li, Y.G. (2015), "Finite element analysis of the soil pressure in sandy soil at the top of pipe culvert", *Appl. Mech. Mater.*, https://doi.org/10.4028/www.scientific.net/AMM.744-746.1077.

Esmaeili-Falak, M. and Sarkhani Benemaran, R. (2024), "Application of optimization-based regression analysis for evaluation of frost durability of recycled aggregate concrete", *Struct. Concrete*, https://doi.org/10.1002/suco.202300566.

Esmaeili-Falak, M. and Sarkhani Benemaran, R. (2024), "Ensemble extreme gradient boosting based models to predict the bearing capacity of micropile group", *Appl. Ocean Res.*, 104149. https://doi.org/10.1016/j.apor.2024.104149.

Evans, C.H. (1983), *An examination of arching in granular soils (Doctoral dissertation, Massachusetts Institute of Technology).*

Hassankhani, E. (2020), *Applied Pressure on Box Culverts Buried in Rigid Trenches Using Induced Trench Method* [University of Tabriz]. Tabriz, Iran.

Hassankhani, E. and Esmaeili-Falak, M. (2024), "Soil-structure interaction for buried conduits influenced by the coupled effect of the protective layer and trench installation", *J. Pipe. Syst. Eng. Pract.*, https://doi.org/https://doi.org/10.1061/JPSEA2/PSENG-1547.

Hassankhani, E. and Halabian, A.M. (2018), "Parametric study of concrete-face performance in cfrds considering hardening behavior of rockfill material", *Sharif J. Civil Eng.*, **34**(3.1), 37-47. https://doi.org/10.24200/j30.2018.1409.

Hassankhani, E., Moradi, G. and Halabian, A.M. (2016), "Design of a test box to study of buried culverts in trenches", *Proceedings of the 5th International Conference on Geotechnical Engineering and Soil Mechanics.*, Tehran, Iran. https://doi.org/10.12989/gae.2023.34.5.507.

Helwany, S. (2007), *Applied soil mechanics with ABAQUS applications*. John Wiley & Sons. Book.

Hügel, H., Henke, S. and Kinzler, S. (2008), "High-performance Abaqus simulations in soil mechanics", Abaqus User Conference.

Jiao, N., Wan, X., Ding, J., Zhang, S. and Liu, J. (2024), "Pipeline deformation caused by double curved shield tunnel in soil-rock composite stratum", *Geomech Eng*, **36**(2), 131-143. https://doi.org/10.12989/gae.2024.36.2.131.

Jin, D., Yang, Y., Zhang, R., Yuan, D. and Kang, Z. (2024), "Effect of the support pressure modes on face stability during shield tunneling", *Geomech Eng*, **36**(5), 417-426. https://doi.org/10.12989/gae.2024.36.5.417.

Johnson, N. (2023), "Soil Structure interaction of corrugated box culvert", http://hdl.handle.net/10222/83281.

Katona, M.G. and Vittes, P.D. (1982), "Soil-structure analysis and evaluation of buried box-culvert designs", *Transport. Res, Record*, **878**, 1-7. http://worldcat.org/isbn/0309034663

Kim, K. and Yoo, C.H. (2005), "Design loading on deeply buried box culverts", *J. Geotech. Geoenviron. Eng.*, **131**(1), 20-27. https://doi.org/10.1061/(ASCE)10900241(2005)131:1(20).

Li, L., Aubertin, J.D. and Dubé, J.S. (2014), "Stress distribution in a cohesionless backfill poured in a silo", *Open Civil Eng. J.*, **8**(1), 1-8. https://doi.org/10.2174/1874149501408010001.

Li, Y., Tang, X., Yang, S.A. and Ding, Y. (2023), "Characterization of face stability of shield tunnel excavated in sand-clay mixed ground through transparent soil models", *Geomech Eng*, **33**(5), 439-451. https://doi.org/10.12989/gae.2023.33.5.439.

Liang, R. and Bayrami, B. (2023), "Estimation of frost durability of recycled aggregate concrete by hybridized Random Forests algorithms", *Steel Compos. Struct.*, **49**(1), 91-107. https://doi.org/10.12989/scs.2023.49.1.091.

Maekawa, K., Zhu, X., Chijiwa, N. and Tanabe, S. (2016), "Mechanism of long-term excessive deformation and delayed shear failure of underground RC box culverts", *J. Adv. Concrete Technol..*, **14**(5), 183-204. https://doi.org/10.3151/jact.14.183.

McAffee, R. and Valsangkar, A. (2005), "Performance of an induced trench installation", *Transport. Res. Record: J. Transport. Res. Board*, (1936), 230-237.

Moradi, G., Hassankhani, E. and Halabian, A.M. (2020), "Investigation of applied earth load on buried box culverts in trenches using induced trench method under embankment pressure", *Sharif J. Civil Eng.*, **35**(4.2), 53-65. https://doi.org/10.24200/j30.2018.5720.2271

Moradi, G., Hassankhani, E. and Halabian, A.M. (2022), "Experimental and numerical analyses of buried box culverts in trenches using geofoam", *Proceedings of the Institution of Civil Engineers-Geotechnical Engineering.*, **175**(3), 311-322. https://doi.org/10.1680/jgeen.19.00288.

Nawel, M. and Salah, M. (2015), "Numerical modeling of two parallel tunnels interaction using three-dimensional finite elements method", *Geomech. Eng.*, **9**(6), 775-791. https://doi.org/10.12989/gae.2015.9.6.775.

Oh, J., Moon, T., Canbulat, I. and Moon, J.S. (2019), "Design of initial support required for excavation of underground cavern and shaft from numerical analysis", *Geomech. Eng.*, **17**(6), 573-581. https://doi.org/10.12989/gae.2019.17.6.573.

Orton, S.L., Loehr, J.E., Boeckmann, A. and Havens, G. (2015), "Live-load effect in reinforced concrete box culverts under soil fill", *J. Bridge Eng.*, **20**(11), 04015003. https://doi.org/10.1061/(ASCE)BE.1943-5592.0000745

Pimentel, M., Costa, P., Félix, C. and Figueiras, J. (2009), "Behavior of reinforced concrete box culverts under high embankments", *J. Struct. Eng..*, **135**(4), 366-375. https://doi.org/10.1061/(ASCE)0733-9445(2009)135:4(366).

Selig, E.T. (1972), "Subsurface soil-structure interaction: A synopsis. Highw", *Res. Rec*, **413**, 1-4.

Spangler, M.G. (1933), *The supporting strength of rigid pipe culverts*: Iowa State College.

Spangler, M.G. and Handy, R.L. (1973), *Soil engineering*: Intext Educational Publishers.

Stone, K. and Newson, T. (2022), "Arching effects in soil-structure interaction", In *Physical Modelling in Geotechnics.*, 935-939. Routledge. Book.

Sukamta, D., Rahardjo, P., Alexander, N. and Wijaya, M. (2023), "Soil-structure interaction of huge RC box culvert under high embankment*", IOP Conference Series: Earth and*

Environmental Science. https://ui.adsabs.harvard.edu/link_gateway/2023E&ES.1249a2003S/doi:10.1088/1755-1315/1249/1/012003.
Sun, L., Hopkins, T.C. and Beckham, T.L. (2011), "Long-term monitoring of culvert load reduction using an imperfect ditch backfilled with geofoam", *Transport. Res. Record: J. Transport. Res.Board*, **2212**(1), 56-64.
Sun, X., Dong, X., Teng, W., Wang, L. and Hassankhani, E. (2024), "Creation of regression analysis for estimation of carbon fiber reinforced polymer-steel bond strength", *Steel Compos. Struct.*, **51**(5), 509-527. https://doi.org/10.12989/scs.2024.51.5.509.
Tadros, M.K. (1986), *Cost-effective Concrete Box-culvert Design*: University of Nebraska-Lincoln, Department of Civil Engineering.
Tafreshi, S.M., Mehrjardi, G.T. and Dawson, A. (2012), "Buried pipes in rubber-soil backfilled trenches under cyclic loading", *J. Geotech. Geoenviron. Eng*., **138**(11), 1346-1356.
Terzaghi, K. (1943), *Theoretical soil mechanics*, Wiley New York. book
Terzi, N.U., Erenson, C. and Selcuk, M.E. (2015), "Geotechnical properties of tire-sand mixtures as backfill material for buried pipe installations", *Geomech. Eng.*, **9**(4), 447-464. https://doi.org/10.12989/gae.2015.9.4.447.
Wang, J. and Huang, J. (2021), "Soil pressure reduction by including geofoam: A numerical study", *Int. J. Geosynth. Ground Eng.*, **7**(2), 1-12. https://doi.org/10.1007/s40891-021-00268-9.
Wei, H.W., Yang, X.L. and Yu, Z.H. (2012), "Performance of soil pressure on the culvert under high-backfill reinforced with geosynthetics", *Adv. Mater. Res.*, **368**(5), 1955-1960. doi:10.4028/www.scientific.net/AMR.368-373.1955.
Wu, L., Li, M., Zhang, J.A., Wang, Z., Yang, X. and Bian, H. (2024), "Deep learning-based AI constitutive modeling for sandstone and mudstone under cyclic loading conditions", *Geomech. Eng.*, **37**(1), 49-64. https://doi.org/10.12989/gae.2024.37.1.049.
Xenaki, V. and Athanasopoulos, G. (2001), "Experimental investigation of the interaction mechanism at the EPS geofoam-sand interface by direct shear testing", *Geosynth. Int.*, **8**(6), 471-499. https://doi.org/10.1680/gein.8.0204.
Yoo, M., Kwon, S.Y. and Hong, S. (2022), "Dynamic response evaluation of deep underground structures based on numerical simulation", *Geomech. Eng.*, **29**(3), 269-279. https://doi.org/10.12989/gae.2022.29.3.269.
Zheng, J. and Li, L. (2024), "Experimental and numerical study on the earth pressure coefficient in a vertical backfilled opening", *Geomech Eng*, **36**(3), 217-229. https://doi.org/10.12989/gae.2024.36.3.217.

GC